Talanta Open 11 (2025) 100417

Contents lists available at ScienceDirect

Talanta Open

journal homepage: www.sciencedirect.com/journal/talanta-open

Nano-MIP based SPR sensor for tetracycline analysis in milk sample

Monireh Bakhshpour-Yücel, Melike Küçük, Elif Tümay Özer, Bilgen Osman *

Bursa Uludag University, Department of Chemistry, Faculty of Arts and Science, Bursa, Turkey

ARTICLE INFO

Keywords:
Surface plasmon resonance
Molecularly imprinted nanoparticles
Tetracycline
Food safety
Human safety

ABSTRACT

Recent advancements in sensor technology have enabled the detection of antibiotics in food, ensuring human safety. In this study, we developed a surface plasmon resonance (SPR) sensor based on molecularly imprinted nanoparticles (MINps) for the real-time, sensitive, and in-situ detection of tetracycline (Tc). Firstly, Tc-imprinted nanoparticles (Tc-MINps) were synthesized using microemulsion polymerization. Then, the Tc-MINps were coated onto a bare gold SPR chip to develop the Tc-MINps SPR sensor. The sensor's performance was evaluated by detecting Tc in aqueous solutions. The results demonstrated a highly selective binding of Tc to the nanocavities on the surface of the Tc-MINps SPR sensor. The relationship between Tc molecules and the SPR sensor was analyzed at 0.5–20 mg/L Tc concentrations (pH 5.0). The Langmuir isotherm model was identified as the most appropriate binding model, indicating monolayer adsorption. The selectivity of the Tc-MINps SPR sensor was investigated using oxytetracycline, ciprofloxacin, and amoxicillin due to their structural similarity. The selectivity coefficients were determined as 5.54 for oxytetracycline, 23.66 for ciprofloxacin, and 28.39 for amoxicillin. Additionally, the limit of detection (LOD) for the Tc-MINps SPR sensor for Tc analysis in milk was found to be 0.45 mg/L, while the LOD for the HPLC method was 0.55 mg/L. The developed SPR sensor is suitable for Tc detection in milk due to its advantages, such as real-time monitoring, low cost, high selectivity, and reusability.

1. Introduction

Milk, among the most consumed foods in the world, is an important source of essential nutrients since it is rich in proteins, fat, carbohydrates, vitamins, minerals and water [1,2]. Despite this richness, milk is described by some as ‘‘white poison’’ because it can contain many harmful components such as blood, hormones, and antibiotics [1]. In particular, the presence of antibiotics in milk is a concern for consumers. Over 60 thousand tons of antibiotics are used in livestock farming worldwide yearly [3]. Antibiotics are not only used in the primary treatment line, such as mastitis, pneumonia, bacterial diarrhea, and bacterial arthritis for infected animals but are also used to increase feed efficiency and growth rates [2,4]. The excessive and unconscious use of antibiotics in animals can enter the food chain and cause risks to human health. Traces of antibiotic residues found in milk can cause allergic reactions in ultrasensitive consumers, carcinogenic, immunopathological effects, reproductive disorders, and the development of drug-resistant bacteria [2,4,5]. Thus, monitoring the presence of antibiotic residues is very important in controlling the spread of antibiotics and the safety of milk for human consumption [2,5]. For this purpose, antibiotic maximum residue limits (MRL) have been determined by the European Union (Commission Regulation (EU) No. 37/2010) [6].

In recent years, many antibiotic groups, such as β-lactams, fluoroquinolones, sulfonamides, aminoglycosides, and tetracyclines (Tcs), have been detected in milk [3]. Tcs are used more than other antibiotics because of their activity against a wide range of pathogens (Gram--positive and Gram-negative microorganisms), low cost, and relatively low toxicity [7]. According to the EU, in milk, MRL is 100 μg/kg for Tc, oxytetracycline (otc) and chlortetracycline. The limits vary between 4 and 1500 (μg/kg) for different antibiotic groups [3]. Selective and sensitive analytical methods are required to determine the concentration and low levels of antibiotic residues in milk. Several techniques are used, such as high-performance liquid chromatography (HPLC), electrochemistry, capillary electrophoresis, spectrometric, colorimetric, immunoassay, microbiological, aptamer-based assay, biosensors and sensors [2,8–13]. Among these techniques, sensors have become more popular recently because they are less complex, cost-effective, faster, and more straightforward [14].

Sensors are analytical devices that detect chemical and biological molecules. Among the different types of sensors, surface plasmon

* Corresponding author.
E-mail address: bilgeno@uludag.edu.tr (B. Osman).

https://doi.org/10.1016/j.talo.2025.100417
Received 11 December 2024; Received in revised form 31 January 2025; Accepted 1 February 2025
Available online 4 February 2025
2666-8319/© 2025 The Authors. Published by Elsevier B.V. This is an open access article under the CC BY-NC-ND license (http://creativecommons.org/licenses/by-nc-nd/4.0/).

resonance (SPR) sensors are commonly used to detect molecular interactions without labeling. SPR is a powerful optical technique that exploits the interaction between light and electrons at the surface of gold in contact with an aqueous solution [15]. The binding of target molecules to the sensor surface changes the refractive index at the interface, making the SPR sensors particularly useful for detecting biomolecular interactions, such as antigen-antibody, protein-protein, and small-molecule interactions. SPR is used for detection in many areas, such as environmental monitoring (pesticides, metals), biomolecular interactions, medical diagnostics (cancer and protein markers), the pharmaceutical industry, and food quality and safety (pathogens, vitamins, allergens) [16–18]. The detection of antibiotics has become increasingly important due to the rise of antimicrobial resistance and the need to ensure the safety of food and water supplies. SPR sensors have proven to be effective in detecting antibiotics at low concentrations. SPR-based sensors have been used to detect Tc and penicillin residues in milk and other food products. The sensor surface can be functionalized with specific antibodies or molecular receptors that selectively bind to the target antibiotic, generating a measurable shift in the resonance angle as the antibiotic molecules bind [18,19]. To increase the selectivity and sensitivity of sensors, researchers integrated molecularly imprinted polymers (MIPs) with the SPR sensor system. MIPs in SPR-based sensors are particularly valuable for detecting small molecules, such as antibiotics, pesticides, or environmental pollutants, which may not have natural receptors readily available for binding [20,21].

Biological molecules, such as antibodies and enzymes, are widely used in biosensing due to their high specificity, but they suffer from poor stability, high costs, and storage limitations. In addition, there are ethical concerns about the production of antibodies. Producing antibodies for small molecules (haptens) requires carrier proteins and often leads to reduced specificity and batch variability. In contrast, MIPs offer a cost-effective, stable, and highly selective alternative. They provide enhanced binding kinetics and direct imprinting capabilities, making them promising substitutes in biosensing and diagnostic applications. MIPs also offer superior thermal and pH stability, remaining functional at higher temperatures and over the years, whereas biological molecules degrade within months and denature around 70 °C. Furthermore, MIPs are cost-effective, easier to store, and achieve high specificity and affinity (nM to pM range), making them strong alternatives to antibodies. The size of MIPs also plays a crucial role in their binding efficiency; nanosized MIPs provide faster binding kinetics and better diffusion in complex matrices due to their increased surface area, whereas larger MIPs may have higher binding capacity but slower mass transfer [22]. Consequently, nanosized MIPs offer a promising alternative by directly imprinting the target molecule, eliminating the need for carrier proteins and avoiding the associated specificity and affinity issues.

Due to the milk matrix's complexity and Tc's trace level, some sample preparation steps, such as sample pre-treatment, extraction, cleanup, etc., must be applied before instrumental analysis [23]. MIPs provide high affinity and selectivity against target analytes, enabling easy separation and enrichment of analytes at low concentrations for complex matrices. MIPs are prepared based on creating specific recognition sites in cross-linked polymer networks with appropriate shapes, sizes, and functional groups toward the template molecule. MIPs have excellent properties such as ease of preparation, low cost, physical durability, chemical inertness, significant reusability, long storage life, and resistance to high pressure and temperatures [24–26]. MIPs have been developed in many morphologies and sizes, such as monoliths, spherical particles, nanoparticles, flat membranes, and macro-/micro-/nanosized [27]. MIP nanoparticles have unique properties such as small size, high surface area, easy template removal, rapid binding kinetics, good dispersion, and handling ability, which have led to their application in many areas (biomedical, food, agriculture, energy production) [28]. MIPs in the molecular recognition layer of SPR sensors provide high selective recognition of the target analyte, high sensitivity, and a significant decrease in the detection limit.

In this work, a SPR sensor based on Tc-imprinted nanoparticles (Tc-MINps) was developed to use selective Tc detection in aqueous medium and milk samples. N-methacryloyl-l-glutamic acid methyl ester (MAGA) was used as a functional monomer to prepare the Tc-MINps. Also, the non-imprinted nanoparticles (NINps) SPR sensor was designed as a control sensor system. Tc sensing was achieved at different concentrations, and the selectivity of the system was tested using competitor molecules such as otc, ciprofloxacin (cip), and amoxicillin (Amox). This study aimed to detect Tc utilizing the molecular imprinting technique in the SPR optical sensor, which enables real-time, label-free, and quantitative detection of molecular interactions by detecting changes in the refractive index.

2. Materials and methods

2.1. Materials and instrumentations

L-glutamic acid 5-methyl ester, methacryloyl chloride, ammonium persulfate (APS), Tc, otc, Amox and cip were purchased from Sigma. Poly(vinyl alcohol) (PVA) (MW: 100,000) was supplied from Aldrich. Ethylene glycol dimethacrylate (EGDMA), hydroxyethyl methacrylate (HEMA) and all other chemicals were supplied from Merck. All reagents were analytical and HPLC grade in the experiments. Ultrapure water was provided from the Elga Flex3 water purification system.

A Mettler Toledo pH meter (Mettler-Toledo AG, Schwerzenbach, Switzerland) was used to adjust the pH of the solutions. The absorbance values were measured by a UV spectrophotometer (Perkin Elmer Lambda 35, USA). An Agilent 1200 series HPLC system (Agilent, Palo Alto, CA) and a G-1315B diode array detector (DAD) were used for HPLC analyses. Separations were performed using an Agilent Zorbax 300SB-C18 (250 mm, 4.6 mm ID, 5 μm) column.

2.2. Synthesis and characterization of tc-minps, and NINps

MAGA was used as a functional monomer to prepare Tc-MINps. The procedure of MAGA synthesis was given in a previous study [29]. Tc-MINps were synthesized with microemulsion polymerization, as presented in our earlier study [30]. Firstly, the organic phase was prepared by mixing MAGA, HEMA, EGDMA, and Tc (1:0.04:1:9) overnight. PVA, SDS, and $NaHCO_3$ were dissolved in 2.5 mL deionized water for the first aqueous phase. The second aqueous phase was prepared by dissolving equal amounts of PVA and SDS (25 mg) in 50 mL of water. The organic phase was added to the first aqueous phase and mixed with a homogenizer (IKA T 25 Digital Ultra-Turrax) for 20 min (20.000 rpm). After that, the mixture was added to the second aqueous phase. The resulting mixture was stirred at 60 °C for 24 h after adding $NaHSO_3$ and APS. The Tc-imprinted nanoparticles were separated through an ultracentrifuge (Beckman coulter) (18.000 rpm, 1 h) and washed with alcohol and water to remove unreacted substances. The template molecule (Tc) was removed by incubating Tc-MINps with methanol: acetic acid (9:1) mixture several times. The NINps were also prepared using the same procedure without adding Tc in the organic phase.

The chemical structure of Tc-MINps was studied by FTIR spectrometer (Perkin Elmer, Spectrum 100, USA). The morphology of the nanoparticles was examined using a scanning electron microscope (SEM) (Jeol, JEM 1200EX, Tokyo, Japan) and high contrast transmission electron microscopy (HC-TEM) (FEI Tecnai G2 Spirit BioTwin, USA). The elemental composition of the nanoparticles was investigated using an elemental analyzer (Costech ECS 4010, USA). The surface charge and electro kinetic behavior of nanoparticles were performed using Zeta potential measurements (Malvern Zetasizer, UK).

2.3. pH effect on TC adsorption onto Tc-MINps

TC adsorption studies from aqueous solutions with Tc-MINps were carried out with a batch system to investigate the effect of pH on Tc

adsorption. To determine the effect of pH on adsorption, Tc solutions with pH values ranging from 2.0 to 9.0 were prepared. 0.01 M HCl and 0.01 M NaOH solutions were used to adjust the pH values of Tc solutions (5 mg/L). A specific volume (20 mL) of Tc solution was mixed with the nanoparticles and stirred at room temperature for 24 h to calculate the amount of Tc adsorbed by Tc-MINps (Q, mg Tc /g nanoparticles). The Tc concentration in aqueous solutions before and after adsorption was calculated through absorbance measurements at 358 nm wavelength in a UV spectrophotometer (Perkin Elmer) through a calibration curve. Tc adsorption studies were carried out using both Tc-MINps and NINps. The amount of Tc adsorbed per 1 g of nanoparticles, Q (mg Tc/g nanoparticles), was calculated using Eq. (1) [31],

$$qe = [(C_o - C_e) \times V]/m \quad (1)$$

where qe represents the amount of mg Tc adsorbed per g nanoparticles (mg/g); C_0 and C_e represent the Tc concentration in the aqueous solution before and after adsorption (mg/L), respectively; V represents the volume of the aqueous solution (mL) and m represents the mass of nanoparticles (g).

2.4. Preparation and characterization of Tc-MINps and NINps SPR sensor chips

To immobilize the nanoparticles onto the gold SPR surface and achieve homogeneous immobilization, the following procedure was applied: First, the surface of the bare gold SPR chip was cleaned via a piranha solution (3 H_2SO_4/1 H_2O_2). It was followed by washing with % 50 ethanol and deionized water. Finally, a stream of N_2 gas was used to dry the surface of the SPR chip. Then, 5 mg Tc-MINps were dispersed into 100 mL of deionized water and sonicated for 15–20 min (Bandelin Sonorex), after which 15 μL of Tc-MINps solution was dropped and spin-coated onto the bare gold SPR chip surface. The Tc-MINps SPR chip was incubated in a vacuum oven (Binder) at 37 °C for 6 h to allow the fixation of Tc-MINps onto the SPR chip surface. The same procedure was followed to prepare the NINps SPR chip [32,33]. The preparation of the SPR sensor is shown in Scheme 1, illustrating the process involved in the preparation of the SPR sensor. It outlines the key steps and components required to develop the SPR sensor for detecting Tc molecules.

The characterization of the bare, NINps, and Tc-MINps SPR chips was performed using a water contact angle (WCA) measurement system (Attention KSV Instrument, Espoo, Finland) and optical profilometer (Zeta Instruments, San Jose, CA, USA). The WCAs of SPR chips were determined via the sessile drop method, where a single drop of water was placed on the surface of the SPR chips. The WCA of the bare, NINps, and Tc-MINps SPR chip surfaces were measured in five different areas capturing 40 different images. The thickness of the Tc-MINps coating on the SPR chip was measured using optical profilometer that were carried out at three different regions on the Tc-MINps SPR chip.

2.5. Kinetic studies with Tc-MINps SPR sensor

Kinetic studies were conducted via the SPR-Imager II system (GWC Technologies, Wisconsin, USA). The calibration curve was prepared using Tc solutions in the concentration range of 0.5–20 mg/L (pH 5.0). The solutions were prepared with 0.1 M acetate buffer. Each Tc solution was analyzed separately using the SPR sensor system. Equilibrium was reached when all nanocavities in the Tc-MINps SPR sensor surface were saturated. A desorption solution (methanol: acetic acid, 9:1) was used to remove the Tc molecules. For each Tc solution, the percentage change in reflectance (% ΔR) over time was visualized from the sensorgram. The same kinetic analyses were conducted using the NINps SPR sensor as a control. In each experimental cycle of the SPR sensor system, the first step involved passing the pH 5.0 buffer solution (0.1 M acetate buffer) through the system for 180–200 ss to establish equilibrium. Then, Tc solutions at various concentrations were passed from the SPR chip surface, and real-time signal changes were recorded and monitored for 500 ss. After reaching equilibrium, the desorption solution was passed through the system for 100 ss to remove the Tc molecules from the nanocavities. At the end of each experiment, the SPR sensor surface was cleaned with deionized water for 180 ss to prepare it for subsequent analyses. The limit of detection (LOD) value was determined using the SPR sensor data. The LOD was calculated using the equation of 3s/m, where s represents the standard deviation of the SPR signal (ΔR) obtained for the minimum Tc concentration that causes a SPR sensor response, and m denotes the slope of the calibration curve [34].

The experimental data were fitted with equilibrium and isotherm models. Langmuir, Freundlich and Langmuir-Freundlich isotherm models were applied to determine the type of binding site interactions. These models are commonly used in studies involving MIPs, making them particularly suitable for analyzing the data obtained in this experiment. Additionally, the Langmuir-Freundlich isotherm model was employed to provide insights into the heterogeneity of binding sites across a wide concentration range up to saturation. The following equations determined the interaction equilibrium constant and the isotherm model governing the interaction between the SPR sensor and Tc molecules [35].

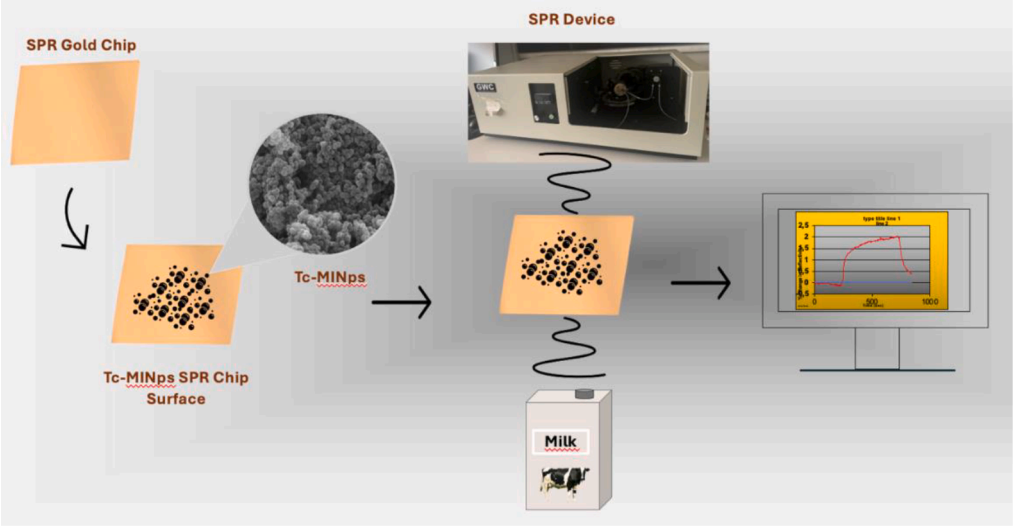

Scheme 1. The schematic representation of the steps involved in preparing the Tc-MINps SPR sensor.

$$Scatchard: \Delta R_{eq}/[C] = K_A(\Delta R_{max} - \Delta R_{eq}) \quad (2)$$

$$Langmuir: \Delta R = \{\Delta R_{max} / [C] / (K_D + [C])\} \quad (3)$$

$$Freundlich: \Delta R = \Delta R_{max}[C]1/n \quad (4)$$

$$Langmuir - Freundlich: \Delta R = \{\Delta R_{max}[C](1/n) / K_D + [C]1/n\} \quad (5)$$

Here, ΔR_{max}, maximum signal shift; ΔR_{eq}, the signal at equilibrium; [C], analyte concentration (mgL^{-1}); K_A ($1/mgL^{-1}$), binding equilibrium constant; K_D (mgL^{-1}), dissociation equilibrium constant; 1/n, Freundlich surface heterogeneity index.

2.6. Selectivity studies

The selectivity of the Tc-MINPs SPR sensor was evaluated using otc, cip, and Amox solutions, each prepared separately at a concentration of 20 mg/L in pH 5.0, as competing analytes. Each competitor solution was individually passed through the SPR sensor, and the corresponding sensor responses (sensorgrams) were recorded. Additionally, sensorgrams were obtained for binary mixtures (Tc-Otc, Tc-Cip, and Tc-Amox) and a quadruple mixture (Tc-Otc-Cip-Amox) to further assess the selectivity of the Tc-MINPs SPR sensor. In these mixtures, the concentration of each competitor was maintained at 20 mg/L. Following the adsorption and desorption steps, the sensor surface was washed with deionized water and the buffer solution (pH 5.0) to prepare the SPR sensor for subsequent analyses. The adsorption, desorption, washing, and equilibration steps were repeated three times for each sample. The selectivity coefficient (k), and relative selectivity coefficient (k') were calculated using mathematical models based on the data obtained.

The equation for K_d is given below; [33]

$$K_d = [C_i - C_f / C_f] \times V/m \quad (6)$$

where K_d represents the distribution coefficient (mL/g) and the initial and final concentrations of the samples (mg/L); V represents the volume of solution used (mL), and m is the weight of the Tc-MINPs (g). In the SPR sensor approach, the concentration and mass parameters are converted for practical use. The rationale for this approach is as follows: there is no significant difference between the initial and final concentrations; the mass of the Tc-MINPs cannot be accurately determined; and the concentration is linearly related to the resonance shift. Under these conditions, this equation can be applied to calculate the selectivity coefficient (k) and relative selectivity coefficient (k'). The following equations can be used to determine the imprinting selectivity [33].

$$k = \Delta R\%_{template}/\Delta R\%_{competitor} \quad (7)$$

$$k' = k_{Tc-MINps\,SPRsensor}/k_{NINpsSPRsensor} \quad (8)$$

2.7. Reusability and repeatability studies

Reusability is a critical property of any sensor system. It directly impacts the cost-effectiveness, efficiency, and sustainability of the sensor analysis. The reusability of the Tc-MINPs-SPR chip without significant loss of performance ensures that experiments can be conducted repeatedly with minimal expense for SPR chip replacement. The reusability also vital for the practicality and value of the designed SPR sensors. By the way, the stable Tc-MINPs onto the SPR sensor show hardiness to harsh conditions, such as extreme pH and ionic strength, which may affect the SPR sensor performance. In this study, the reusability and stability of the Tc-MINPs SPR sensor were evaluated by consecutively interacting a Tc solution prepared at a concentration of 50 mg/L (pH 5.0) with the sensor surface six times over three consecutive days. After each analysis, a desorption solution consisting of methanol and acetic acid (9:1) was used to remove the Tc molecules for free Tc binding sites, and the subsequent analysis was then performed. Tc solutions were analyzed via the Tc-MINPs SPR sensor for two times in one day. The Tc-MINPs SPR sensor was stored at room temperature during the experiments.

2.8. Tc analysis in milk via the Tc-MINPs SPR sensor

The pasteurized milk samples were purchased from a local market in Bursa, Turkey, and used to test the applicability of the developed SPR method for Tc analysis on a real sample. Milk protein precipitation was achieved using the procedure including acetone with minor modifications. According to the pre-sample preparation method, 5 mL of homogenized milk sample was added to 10 mL of acetonitrile. After vortex mixing of the solution for 2 min, the sample was centrifuged for 20 min at 10,000 rpm. Then, the supernatant was carefully transferred to a new centrifuge tube, filtered (0.22 μm filter membrane), and used for matrix-matching calibration and developing the new SPR method.

At optimal conditions, all analytical performance parameters of the developed SPR procedure, including the relative standard deviation (RSD, %) at three concentration points (1, 5, 10 mg/L), LOD, limit of quantification (LOQ), linear range and correlation coefficient, were determined. The LOD was calculated using the equation 3s/m, where s represents the standard deviation of the lowest SPR signal (ΔR), and m denotes the slope of the calibration curve [33–35]. In addition, the milk sample was analyzed using both HPLC analysis and Tc-MINPs SPR sensor for method verification. In the HPLC method, acetonitrile and 1 % formic acid were used as a mobile phase A and a mobile phase B, respectively. The separation was carried out in gradient flow. The experimental conditions: flow rate: 1 mL/min; injection volume: 10 μL; column temperature: 22 °C; the wavelength of the PDA detector: 358 nm; and total analysis run time: 21 min. Tc was eluted at 14.342 min in the column [36].

3. Results and discussion

3.1. Morphological and chemical properties of the Tc-MINPs

MIPs enable the preparation of highly sensitive sensors. One of the most critical factors determining the sensitivity of a MIP-based sensor is the selectivity of MIP to the target analyte. Nano-sized MIPs enable high sensor signals due to their high surface areas. Therefore, the size and morphological structure of MIP nanoparticles used in sensors are of great importance. Morphological analyses of Tc-MINPs performed by SEM (Fig. 1A) and HC-TEM (Fig. 1B) clearly showed that the nanoparticles are perfectly spherical, and the average size of the nanoparticles is about 80 nm. Due to the high surface area/volume ratio and small size, the prepared Tc-MINPs provided a high binding capacity.

The Tc-MINPs were chemically characterized via FTIR analysis. The FTIR spectrum of Tc-MINPs is given in Supplementary Information as Fig. SI1. The broad absorption band in the 3200–3500 cm^{-1} frequency range is mainly due to the stretching of –OH groups of HEMA used as a comonomer. The adsorption bands were observed for the C–H stretch at 2951 cm^{-1}, the ester carbonyl group at 1721 cm^{-1}, and the amide carbonyl group at 1667 cm^{-1} [30]. These characteristic bands show that MAGA (functional monomer) was incorporated into the polymeric structure, and the Tc-MINPs were successfully synthesized. The chemical structures of MAGA and Tc are provided in Fig. SI2. The elemental analysis of the Tc-MINPs demonstrated that the nanoparticles included 58.90 ± 0.45 % C, 6.90 ± 0.06 % H, and 0.25 ± 0.03 % N ($n = 4$). The N atom in the composition resulted from MAGA in the Tc-MINPs structure used as a functional monomer. These results clearly showed that the MAGA monomer was successfully incorporated into the structure.

3.2. Effect of pH on Tc adsorption onto Tc-MINPs

The effect of pH on Tc adsorption onto Tc-MINPs was investigated via batch adsorption studies. The solutions containing Tc at a

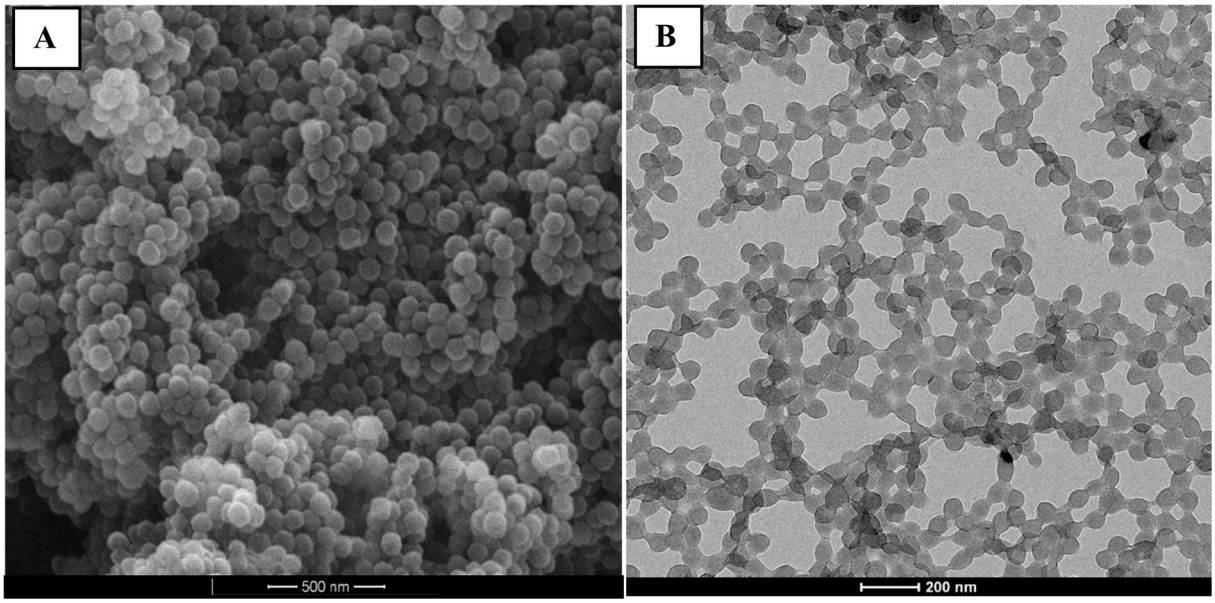

Fig. 1. A.) SEM and B.) HC-TEM images of Tc-MINps.

concentration of 5 mg/L at different pH values (2.0–9.0) were used for adsorption studies. The Zeta potential of the Tc-MINps was also determined in the pH range of 2.0 to 9.0. The obtained results for Zeta potential and pH effect are given in Fig. 2A and B, respectively. The Zeta potential of the Tc-MINps nanoparticles decreased with increasing pH. Zeta potential has a negative value at the pHs higher than 2.0. The amount of adsorbed Tc increases when the pH rises from 3.0 to 5.0, while it shows a decreasing trend towards higher pHs (Fig. 2B). The highest adsorption capacity (6.85 mg Tc/g nanoparticle) was obtained at pH 5.0. Tc molecule has three different ionizable groups with pKa values of 3.3, 7.68, and 9.68. In aqueous solution, cation species (pH < 3.3), zwitter ion species (3.3 < pH < 7.68) or anion species (pH > 7.68) are formed in different pH environments. Tc exists in the cationic form (TCH_3^+) when pH <3.3 and in the form of zwitterion ($TCH_2^\pm$) between pH 3.3 – 7.7. While it is a monovalent anion (TCH^-) between pH 7.7 and 9.7, it is in the form of a divalent anion (TC^{2-}) when pH > 9.7 [37]. The maximum adsorption capacity at pH 5.0 may be due to the electrostatic interaction between the ionized groups of Tc and negatively charged MAGA. The pKa value of the carboxylic acid group of MAGA is 4.3. At pH 5.0, the carboxylic acid group loses a proton and becomes a carboxylate ion. At pH 5.0, the dimethyl amino group of Tc is positively charged and interacts electrostatically with the negatively charged carboxylate of the MAGA monomer. In addition, MAGA can form hydrogen bonds with the phenolic diketone group and the –OH groups of the tricarbonylamide group. Since the binding capacity is maximum at pH 5.0, the SPR sensorgrams were recorded with Tc solutions prepared using pH 5.0 acetate buffer in the following studies.

3.3. Surface properties of the Tc-MINps SPR sensor chip

One of the most essential properties of the SPR sensor surfaces is wettability because the SPR sensing required to formation of plasmons on the Au surface. The wettability of the bare Au, Tc-MINps, and NINps SPR chip surface was determined by measuring the WCA of the surfaces. The bare Au SPR surface displayed a WCA of 91.98±0.64°, showing a relatively high degree of hydrophobicity. Following the immobilization of NINps and Tc-MINps onto the gold SPR surface, the WCA of the NINps and Tc-MINps SPR chip surfaces decreased to 74.51±0.32° and 71.37 ±1.12°, respectively. The decrease in WCA reflected the modification of the Au SPR surface with the nanoparticles. The observed reduction in WCA suggested an increase in surface hydrophilicity of both surfaces, probably resulting from the roughness caused by the nanoparticles. The

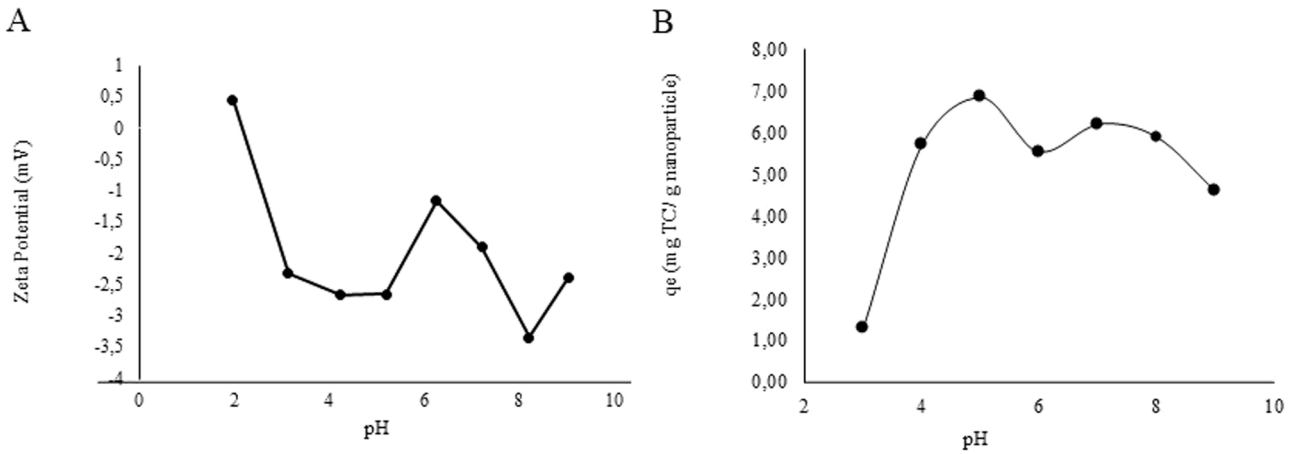

Fig. 2. A.) Zeta potential of the Tc-MINps at different pHs, B.) The pH effect on Tc adsorption onto Tc-MINps (V: 20 mL sample; 1.98 mg Tc-MINps, Concentration: 5.0 mg/L; Time: 24 h., Temperature: 25 °C).

WCA images of the bare Au, NINps, and Tc-MINps SPR chips are shown in Fig. 3A–C.

The thickness of the recognition layer immobilized onto the SPR chip surface was very important since the penetration depth in conventional SPR is lower than 300 nm [38]. The thickness of the Tc-MINps coating on the Au surface was measured as 250 ± 1.1 nm by optical profilometer, which is proper for penetration of plasmons in SRP sensing. Optical profilometer images of the Tc-MINps SPR chip, recorded at different magnification ratios, are presented in Fig. 3D and E. The results clearly demonstrated that Tc-MINps were homogeneously coated onto the SRP chip.

3.4. Tc-MINps SPR sensor method for Tc analysis

The ability of the Tc-MINps SPR sensor to detect Tc in aqueous solution was investigated at different Tc concentrations. For this purpose, the concentration of Tc was incrementally varied between 0.5 and 20 mg/L (pH 5.0). Fig. 4A shows the prepared sensorgrams (% ΔR vs time) for Tc solutions at different concentrations. The SPR sensorgrams showed the cycles of equilibrium, binding, dissociation, and re-equilibration. The increase in ΔR% with increasing Tc concentration showed that Tc molecules interacted with the target-specific cavities (binding sites) of the Tc-MINps on the SPR sensor surface, causing a sensor response. The binding sites were become saturated, eventually reaching equilibrium. As shown in Fig. 4A, the SPR response was linearly increased with increasing Tc concentration (R^2:0.9542). The equilibrium binding graph is shown in Fig. 4B. The data obtained in kinetic studies enabled the calculation of the constants and values, including ΔR_{max}, R^2, K_A, and K_D (Table 1). The graphs for the Langmuir, Freundlich, and Langmuir-Freundlich isotherm models are depicted in Fig. 4C–E, respectively. The Langmuir-Freundlich isotherm model was the most suitable binding model (R^2:0.9965). The LOD and LOQ values of the Tc-MINps SPR sensor were 0.45 mg/L and 1.51 mg/L, respectively, which displayed high sensitivity and selectivity for the Tc molecules. The results showed that the sensor enabled the obtaining of sensitive and reproducible measurements, making it suitable for TC detection in real samples.

3.5. Selectivity studies

The selectivity of the Tc-MINps SPR sensor was investigated using Otc, Cip, and Amox as competitor molecules because they can exist together with Tc in various samples such as tap water, waste water, milk, etc. Kinetic analyses were initially performed by introducing individual competitor solutions (20 mg/L) into the SPR system. Subsequently, binary mixtures (Tc-Otc, Tc-Cip, and Tc-Amox) and a quadruple mixture (Tc-Otc-Cip-Amox) were sequentially introduced for further kinetic evaluation (Fig. 5A). The resulting SPR sensorgrams exhibited no significant differences, indicating that the binding interactions between the Tc-MINPs and Tc remained stable in the presence of different competitor mixtures, highlighting their robustness. Fig. 5B shows the sensor response of the NINps for Tc solution in the 20 mg/L concentration.

The selectivity coefficient (k) and relative selectivity coefficient (k′) were calculated and are summarized in Table 2. The selectivity coefficients for otc, cip, and Amox were calculated as 5.54, 23.66, and 28.39, respectively. High relative selectivity coefficients demonstrated that the Tc-MINps SPR sensor has a high affinity for the Tc molecules.

The observed selectivity enabled the MIPs to bind Tc molecules with high affinity and specificity. In this context, selectivity refers to the polymer's ability to effectively distinguish the target molecule from structurally similar compounds, ensuring precise binding and efficient target identification. This inherent ability of MIPs to selectively recognize and bind specific targets makes them highly valuable in sensor applications, where accurate detection and separation of target molecules from complex mixtures are crucial.

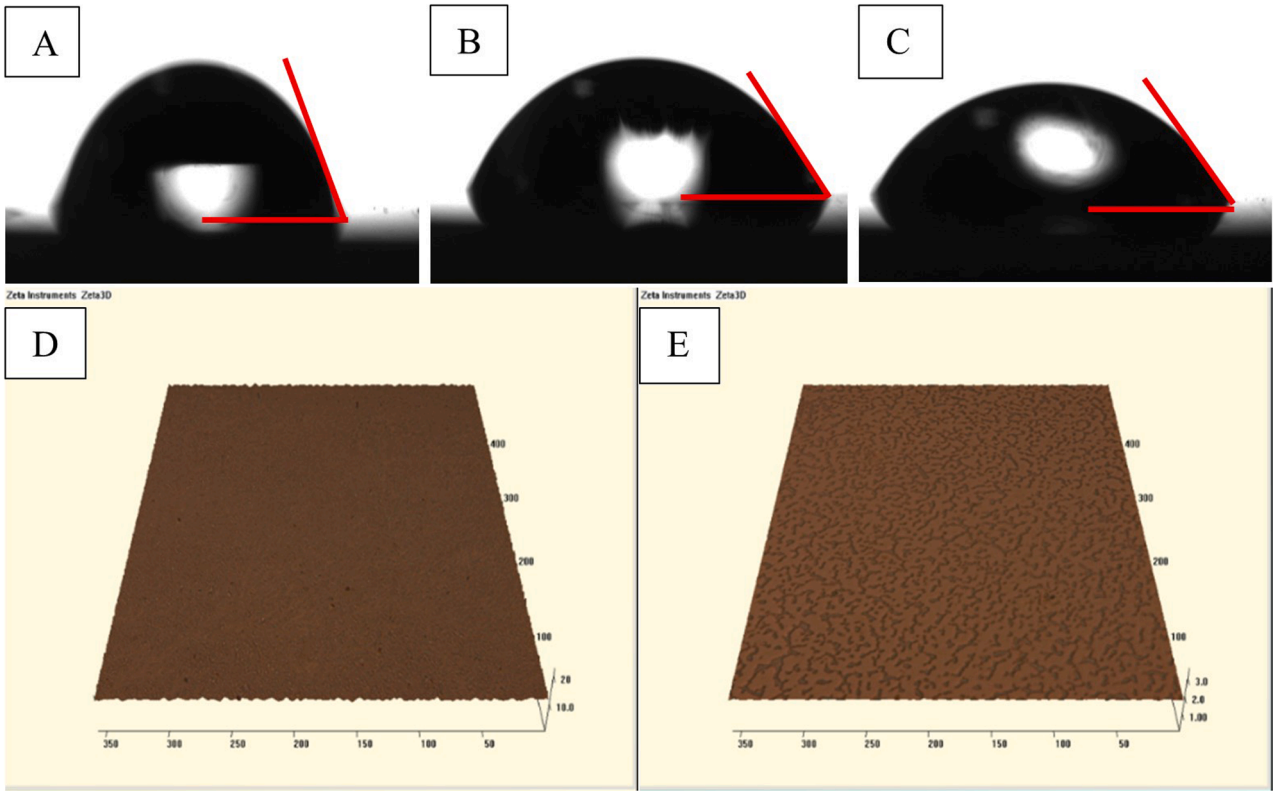

Fig. 3. The WCA of A.) the bare Au, B.) NINps, and C.) Tc-MINps SPR chip images, D.) x20 and E.) x100 optical profilometer images of the Tc-MINps SPR chip.

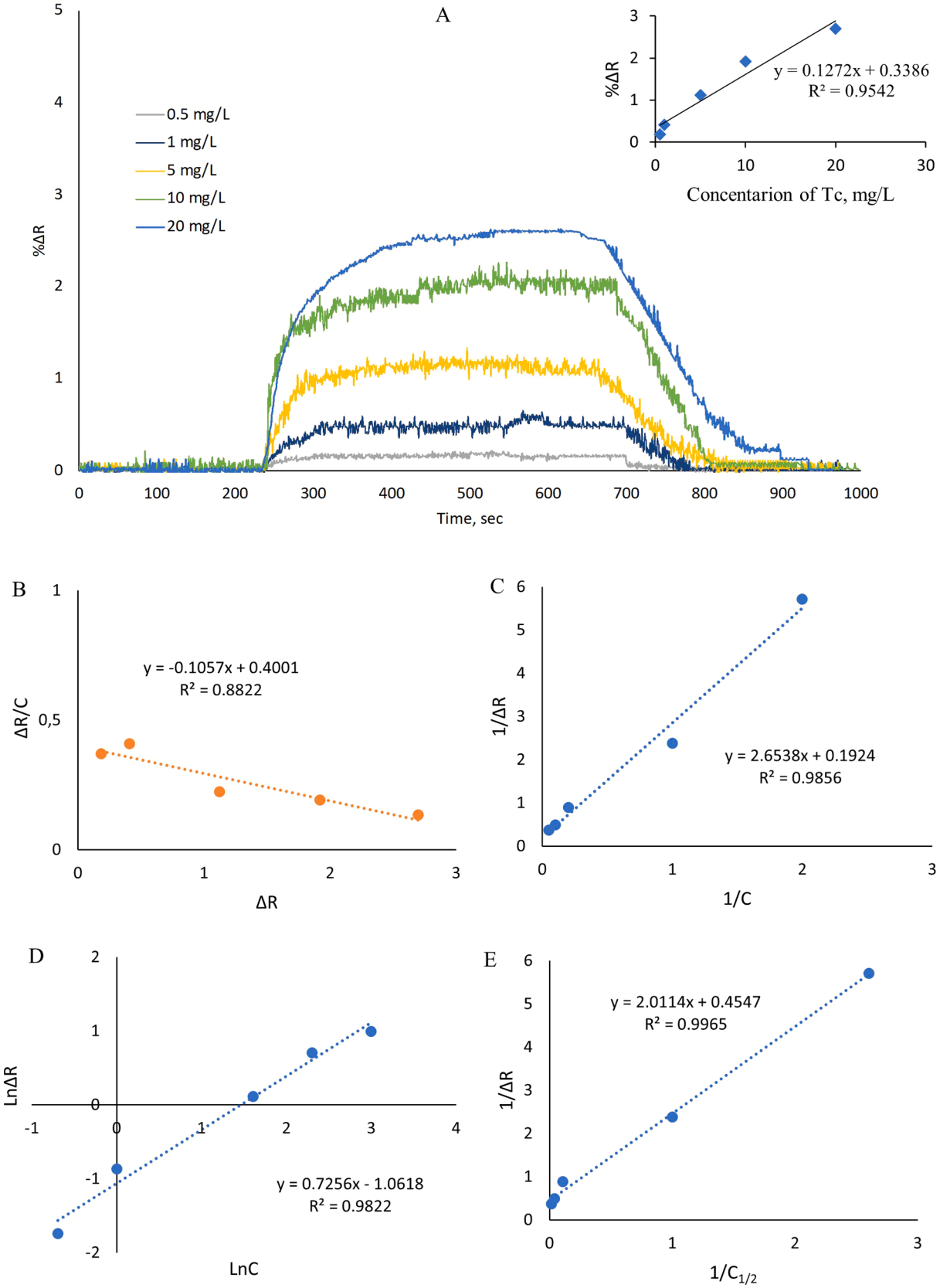

Fig. 4. A.) The real-time response of the Tc-MINps SPR sensor for Tc detection in aqueous solution (Concentration: 0.5–20 mg/L, pH: 5, flow rate: 0.25 mL/min, V: 5 mL, Temperature: 25 °C), The calibration graph for Tc, B.) Equilibrium binding analysis using the Scatchard method, C.) Langmuir, D.) Freundlich, E.) Langmuir-Freundlich isotherm models.

Table 1
Equilibrium binding analysis using the Scatchard method, Langmuir, Freundlich, and Langmuir-Freundlich isotherm models.

Equilibrium analysis, (Scatchard)		*Langmuir*		*Freundlich*		*Langmuir-Freundlich*	
AR_{max}	*3.81*	AR_{max}	*5.19*	AR_{max}	*3.97*	AR_{max}	*2.22*
K_A /(L/mg)	*0.105*	K_A /(L/mg)	*0.510*	*1/n*	*1.37*	K_A /(L/mg)	*0.223*
K_D mg/L	*9.52*	K_D mg/L	*1.98*	R^2	*0.98*	K_D mg/L	*4.46*
R^2	*0.88*	R^2	*0.98*			R^2	*0.99*

3.5. Reusability study

As an essential factor in sensor systems, reusability ensures both cost-effectiveness and sustainability without significant performance loss in analytical applications. The reusability of the Tc-MINps SPR sensor system was investigated with a Tc solution in 50 mg/L concentration at pH 5.0 over three consecutive days. The SPR response was recorded two times within the same day. Fig. 6 shows that the Tc-MINps SPR sensor can be reused successfully without a significant decrease in sensor response (ΔR%). The RSD values were also calculated as 1.44 for the reusability on the same day and 1.72 for the different days. The results showed that the Tc-MINps SPR sensor was reusable and stable, enabling consecutive usage in Tc analysis.

3.6. Tc analysis in milk with the Tc-MINps SPR sensor

The Tc-MINps SPR sensor method was finally applied to milk samples using the optimized and validated method to analyze Tc residue in real samples. The sensorgrams of the Tc-spiked milk samples are shown in Fig. 7. The linear response was obtained in the studied concentration range with a correlation coefficient of 0.979 for milk samples, demonstrating that the developed SPR sensor presented the same performance as the aqueous solution. The analytical figures of merit, including linearity, LOD, LOQ, and relative standard deviation (RSD%) of the calibration curve, were calculated to validate the developed Tc-MINps SPR sensor method (Table 3). The linearity of the developed SPR sensor procedure was wide, and the correlation coefficient (R^2) of the calibration graph was 0.979. Furthermore, the value of LOD was calculated as 0.45 mg/L. The added–found method was used to evaluate the method's accuracy and matrix effect in the milk samples at 0.5, 1, 5,10, and 20 mg/L concentrations in three replicates. HPLC method results were also evaluated to determine the method accuracy and summarized in Table 3. A comparison of the results displayed that the Tc-MINps SPR sensor method can be successfully used for Tc detection in milk samples.

Table 2
The selectivity coefficients (k) for the Tc-MINps and NINps and relative selectivity coefficients (k').

Analyte	*Tc-MINps SPR*		*NINps SPR*		
	ΔR%	*k*	*ΔR%*	*k*	*k'*
Tc	2.61	-	0.102	-	–
Otc	0.42	6.21	0.091	1.12	5.54
Cip	0.109	23.9	0.101	1.01	23.66
Amox	0.091	28.68	0.101	1.01	28.39

When HPLC and sensor results were compared in terms of LOD, it was seen that both methods had values close to each other. A brief comparison of our SPR sensor with other sensor systems is also summarized in Table 4 for detecting Tc in milk. As a result, it is clear that the developed Tc-MINps SPR sensor was comparable or even superior to the previously developed sensors in terms of LOD values for Tc analysis in milk.

Table 4 summarizes the LOD values of different sensor systems, including electrochemical, fluorescent, and SPR sensors, used for Tc detection in milk. In electrochemical sensors, various pre-concentration methods with different incubation times were applied before electrochemical measurements. The high analytical signals obtained can be attributed to the selective adsorption of Tc by different recognition sites, such as a modified carbon paste-MIP electrode in square wave voltammetry [39], an anti-Tc monoclonal antibody immobilized on a carboxyl-functionalized Fe3O4 nanoparticle-modified gold electrode in differential pulse voltammetry [42], a nanomaterial-modified pencil graphite electrode in an impedimetric aptasensor [43], and multi-walled carbon nanotubes in aptasensors [44,49]. Fluorescent and chemiluminescent sensors have also been employed for Tc detection, utilizing molybdenum disulfide and cadmium telluride quantum dots [40], molecularly imprinted polymers on carbon quantum dots [41], vanadium disulfide quantum dots and molybdenum disulfide nanosheets [45], molecularly imprinted polymer-based approaches [47], and metal-organic framework-based sensors [48]. In the study conducted by Gao et al. [46], a fundamentally different approach was employed for the development of an SPR sensor for Tc detection in milk, resulting in a significant difference in the LOD value compared to our study. In their approach, Tc-imprinted magnetic nanoparticles were first used for the adsorption of Tc from the samples and then separated using a magnet. The Tc-adsorbed nanoparticles, dispersed in phosphate-buffered saline solution, were subsequently introduced to an SPR gold chip modified with mercaptoethylamine. The SPR chip modified with mercaptoethylamine was used for the highly sensitive detection of Tc in combination with the extraction of magnetic molecularly imprinted nanoparticles.

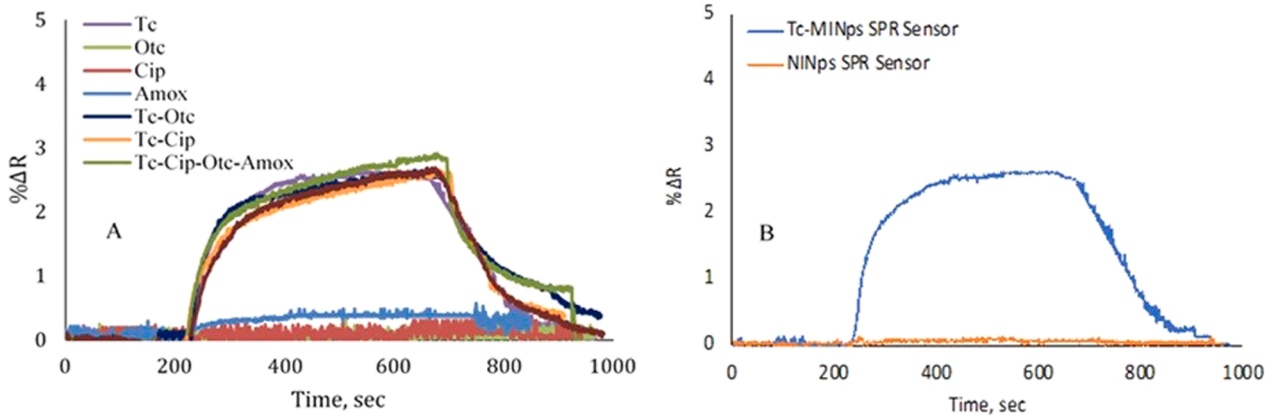

Fig. 5. A.) The selectivity study of the Tc-MINps SPR sensor, (Concentration: 20 mg/L, pH: 5, flow rate: 0.25 mL/min, V: 5 mL, Temperature: 25 °C), B.) The SPR response of the Tc-MINps and NINps for Tc solution (Concentration: 20 mg/L, pH: 5, flow rate: 0.25 mL/min, V: 5 mL, Temperature: 25 °C).

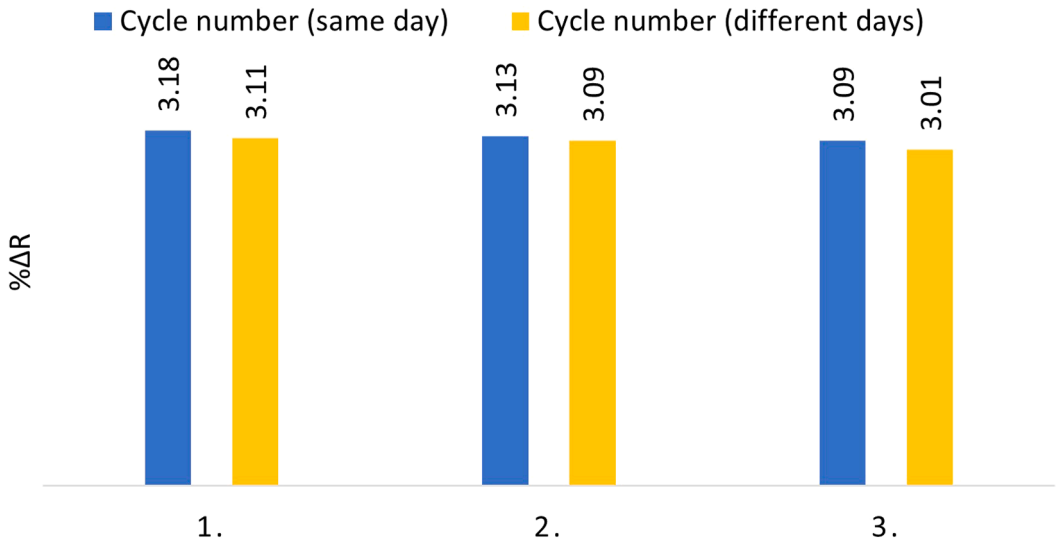

Fig. 6. Reusability of the Tc-MINps SPR sensor three times within the same day and over three consecutive days (Tc solution: 50 mg/L, pH: 5, flow rate: 0.25 mL/min, V: 5 mL, Temperature: 25 °C).

Unlike direct detection of Tc molecules in the sample, this approach relied on detecting Tc-captured magnetic nanoparticles. The thiol group of mercaptoethylamine binds to the chip surface, while the amine group interacts with the hydroxyl or carbonyl groups of the Tc-captured nanoparticles via electrostatic interactions. The limit of detection values obtained from different sensor types and sample preparation methods ranged from 3×10^{-11} μM to 29.25 μM

In our study, Tc-MINps were immobilized directly onto the gold SPR chip surface and used as the sensor's recognition layer. The selectivity and affinity of Tc-MINps directly influenced the SPR sensor response,

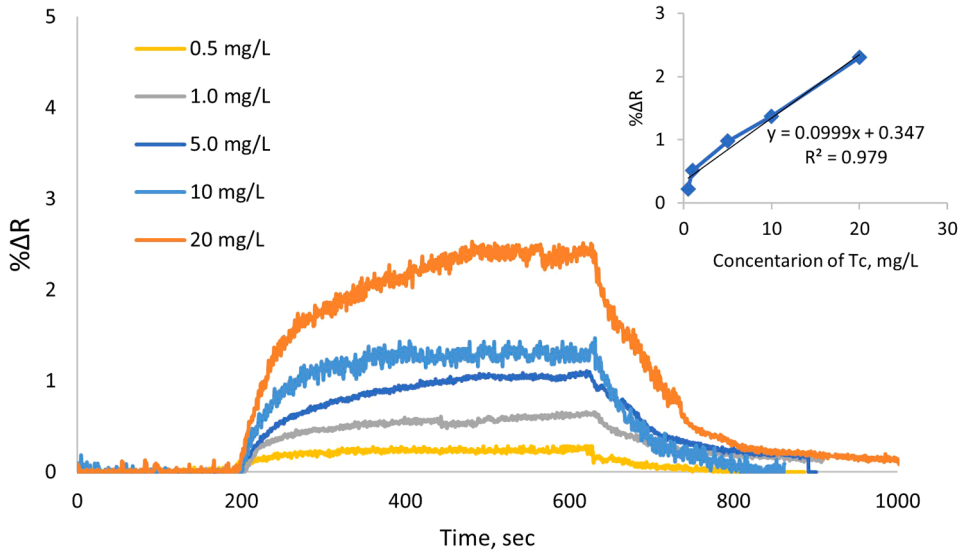

Fig. 7. The sensorgrams for Tc-spiked milk samples in the 0.5–20 mg/L concentration range. Tc spiked into 1/2 diluted blank milk samples (pH: 5.0, flow rate: 0.25 mL/min, V: 5 mL, Temperature: 25 °C).

Table 3
Summary of the figures of merit of the proposed SPR sensor and HPLC methods.

Methods	Linearity (mg/L)	LOD (mg/L)	LOQ (mg/L)	RSD	Added (mg/L)	Found (mg/L)	RSD %	Recovery %
SPR	0.5–20.0	0.45	1.51	3.17	0	N.D.	–	–
					1	1.610± 0.042	2.61	161.0
					5	5.280± 0.053	1.00	105.6
					10	10.210± 0.087	0.85	102.1
HPLC	3.0–20.0	0.55	1.84	3.55	0	N.D.	–	–
					3	3.367± 0.136	4.03	112.24
					5	5.087± 0.051	1.00	101.74
					10	10.089± 0.106	1.05	100.32

Table 4
LODs of different sensor systems for Tc detection of in milk.

Type of sensor	Matrice	Recognation layer	LOD	References
Electrochemical	Market and natural milk	**Magnetic nanoparticles/MIP** Template molecule: TC Monomer: Acrylic acid	0.15 μM	[39]
Fluorescent	Market milk	**Quantum dots** (Molybdenum disulfide and cadmium telluride)	0.0067 μM	[40]
SPR	Urine and milk	**MIP nanoparticles** Template molecule: TC Monomer: Methacrylic acid and itaconic acid	$1.38\ 10^{-8}$ μM	[14]
Fluorescent	Market milk	**Carbon quantum dots/MIP** Template molecule: TC Monomer: 3-aminopropyltriethoxysilane	0.0054 μM	[41]
Electrochemical immunosensor	Market milk	**Chitosan-Magnetic Nanoparticles**	0.072 μM	[42]
Electrochemical biosensor	Milk	**Gold nanoparticles/ Reduced graphene oxide**	3×10^{-11} μM	[43]
An interdigital array microelectrode aptasensor	Market milk	**Multi-walled carbon nanotubes**	1×10^{-3} μM	[44]
Fluorescent	Market milk	**Vanadium(IV) disulfide quantum dots and molybdenum(IV) disulfide nanosheets**	0.135 μM	[45]
SPR	Market milk	**Magnetic MIP nanoparticles** Monomer: Methacrylic acid Template: TC	2.25 nM	[46]
Microtiter chemiluminescence	Market milk	**MIP nanoparticles** Monomer: Methacrylic acid Template: Minocycline	0.0022 μM	[47]
Fluorescent	Market milk	**Metal-organic frameworks/MIP** Monomer: Acrylamide Template: Tc	13.5 μM	[48]
Electrochemical aptasensor	Market milk	**Graphene oxide-systematic evolution of ligands by exponential enrichment**	0.00046 μM	[49]
SPR	Pharmaceutical product	**Ag nanoparticles** Monomer: Acrylamide poly(vinyl pyrrolidone)	29.25 μM	[50]
SPR	Market milk	**Tc imprinted nanoparticles** Monomer: HEMA Template: Tc	1.01 μM	In this study

sensitivity, and selectivity. The SPR sensor developed in this study enabled Tc detection in very small sample volumes without requiring any pre-treatment steps. Moreover, the obtained LOD value (1.01 μM) was comparable to those achieved with other sensor types, while the selectivity of the Tc-MINps SPR sensor was notably higher. In particular, the selectivity coefficient for otc was determined to be 6.21, which is considerably higher than that of many other sensors previously reported in the literature [40,41,47,48].

4. Conclusions

The proposed Tc-MINps SPR sensor system exhibited good sensitivity, wide linearity, simple operation, and high recovery and selectivity for Tc detection in aqueous samples. Additionally, the method was effectively used to analyze Tc in real milk samples. The selectivity of the Tc-MINps SPR sensor system was evaluated by using competitor molecules, such as otc, cip, and Amox. The results showed that the developed Tc-MINps SPR sensor exhibited selectivity for Tc 5.54, 23.66, and 28.39 times greater than for otc, cip, and Amox, respectively, demonstrating the success of the imprinting process. The performance of the SPR sensor was assessed in real-time and the sensor was found to be reusable for Tc detection. Furthermore, the interaction between the sensor and Tc was consistent with the Langmuir-Freundlich adsorption model. This study presents a simple, sensitive, and real-time SPR sensor technology for detecting Tc in milk.

CRediT authorship contribution statement

Monireh Bakhshpour-Yücel: Writing – review & editing, Writing – original draft, Visualization, Software, Methodology, Investigation, Data curation, Conceptualization. **Melike Küçük:** Writing – original draft, Validation, Investigation, Data curation. **Elif Tümay Özer:** Writing – review & editing, Validation, Data curation. **Bilgen Osman:** Writing – review & editing, Resources, Methodology, Data curation, Conceptualization.

Declaration of competing interest

The authors declare that they have no known competing financial interests or personal relationships that could have appeared to influence the work reported in this paper.

Supplementary materials

Supplementary material associated with this article can be found, in the online version, at doi:10.1016/j.talo.2025.100417.

Data availability

Data will be made available on request.

References

[1] P. Rumbold, N. McCullogh, R. Boldon, C. Haskell-Ramsay, L. James, E. Stevenson, B. Green, The potential nutrition-, physical-and health-related benefits of cow's milk for primary-school-aged children, Nutr. Res. Rev. 35 (2022) 50–69, https://doi.org/10.1017/S095442242100007X.
[2] S. Seth, P. Rathinasabapathi, A short review on detection of antibiotics in milk using nanomaterial-based biosensor, Food Anal. Method. 15 (2022) 2181–2192, https://doi.org/10.1007/s12161-022-02291-6.
[3] S. Sachi, J. Ferdous, M.H. Sikder, S.A.K. Hussani, Antibiotic residues in milk: past, present, and future, J. Adv. Vet. Anim. Res. 6 (2019) 315, https://doi.org/10.5455/javar.2019.f350.
[4] D. Bitas, V. Samanidou, Molecularly imprinted polymers as extracting media for the chromatographic determination of antibiotics in milk, Molecules 23 (2018) 316, https://doi.org/10.3390/molecules23020316.

[5] V. Samanidou, S. Nisyriou, Multi-residue methods for confirmatory determination of antibiotics in milk, J. Sep. Sci. 31 (2008) 2068–2090, https://doi.org/10.1002/jssc.200700647.

[6] EU Law, The European Commission Commission Regulation (EU) No. 37/2010, European Union Publications Office, Luxembourg City, Luxembourg, 2016.

[7] J. Kurittu, S. Lönnberg, M. Virta, M. Karp, A group-specific microbiological test for the detection of tetracycline residues in raw milk, J. Agric. Food Chem. 48 (2000) 3372–3377, https://doi.org/10.1021/jf9911794.

[8] R. Urapen, P. Masawat, Novel method for the determination of tetracycline antibiotics in bovine milk based on digital-image-based colorimetry, Int. Dairy J. 44 (2015) 1–5, https://doi.org/10.1016/j.idairyj.2014.12.002.

[9] S. Sivakesava, J. Irudayaraj, Rapid determination of tetracycline in milk by FT-MIR and FT-NIR spectroscopy, J. Dairy Sci. 85 (2002) 487–493, https://doi.org/10.3168/jds.S0022-0302(02)74099-X.

[10] B. Vuran, H.I. Ulusoy, G. Sarp, E. Yilmaz, U. Morgül, A. Kabir, A. Tartaglia, M. Locatelli, M. Soylak, Determination of chloramphenicol and tetracycline residues in milk samples by means of nanofiber coated magnetic particles prior to high-performance liquid chromatography-diode array detection, Talanta 230 (2021) 122307, https://doi.org/10.1016/j.talanta.2021.122307.

[11] C.L. Chen, X. Gu, Determination of tetracycline residues in bovine milk, serum, and urine by capillary electrophoresis, J. AOAC Int. 78 (1995) 1369–1377, https://doi.org/10.1093/jaoac/78.6.1369.

[12] S. Jeong, I. Rhee Paeng, Sensitivity and selectivity on aptamer-based assay: the determination of tetracycline residue in bovine milk, Sci. World J. 2012 (2012) 159456, https://doi.org/10.1100/2012/159456.

[13] W. Thanasarakhan, S. Kruanetr, R.L. Deming, B. Liawruangrath, S. Wangkarn, S. Liawruangrath, Sequential injection spectrophotometric determination of tetracycline antibiotics in pharmaceutical preparations and their residues in honey and milk samples using yttrium (III) and cationic surfactant, Talanta 84 (2011) 1401–1409, https://doi.org/10.1016/j.talanta.2011.03.087.

[14] T. Nawaz, M. Ahmad, J. Yu, S. Wang, T. Wei, A recyclable tetracycline imprinted polymeric SPR sensor: in synergy with itaconic acid and methacrylic acid, New J. Chem. 45 (2021) 3102–3111, https://doi.org/10.1039/D0NJ05364C.

[15] J. Homola, Surface plasmon resonance sensors for detection of chemical and biological species, Chem. Rev. 108 (2008) 462–493, https://doi.org/10.1021/cr068107d.

[16] J. Xu, P. Zhang, Y. Chen, Surface plasmon resonance biosensors: a review of molecular imaging with high spatial resolution, Biosensor. (Basel) 14 (2024) 84, https://doi.org/10.3390/bios14020084.

[17] M. Bakhshpour, A. Denizli, Highly sensitive detection of Cd(II) ions using ion-imprinted surface plasmon resonance sensors, Microchem. J. 159 (2020) 105572, https://doi.org/10.1016/j.microc.2020.105572.

[18] M. Bakhshpour, İ. Göktürk, N. Bereli, F. Yılmaz, A. Denizli, Selective detection of penicillin G antibiotic in milk by molecularly imprinted polymer-based plasmonic SPR sensor, Biomimetics 6 (2021) 72, https://doi.org/10.3390/biomimetics6040072.

[19] V. Safran, İ. Göktürk, M. Bakhshpour, F. Yılmaz, A. Denizli, Development of molecularly imprinted polymer-based optical sensor for the sensitive penicillin G detection in milk, ChemistrySelect 6 (2021) 11865–11875, https://doi.org/10.1002/slct.202103058.

[20] O. Çelik, Y. Saylan, İ. Göktürk, F. Yılmaz, A. Denizli, A surface plasmon resonance sensor with synthetic receptors decorated on graphene oxide for selective detection of benzylpenicillin, Talanta 253 (2023) 123939, https://doi.org/10.1016/j.talanta.2022.123939.

[21] E. Sari, R. Üzek, M. Duman, A. Denizli, Detection of ciprofloxacin through surface plasmon resonance nanosensor with specific recognition sites, J. Biomater. Sci., Polym. 29 (2018) 1302–1318, https://doi.org/10.1080/09205063.2018.1457417.

[22] A.T. Silva, R. Figueiredo, M. Azenha, P.A.S. Jorge, C.M. Pereira, J.A. Ribeiro, Imprinted hydrogel nanoparticles for protein biosensing: a review, ACS Sens. 8 (8) (2023) 2898–2920, https://doi.org/10.1021/acssensors.3c01010.

[23] M. Pérez-Rodríguez, R.G. Pellerano, L. Pezza, H.R. Pezza, An overview of the main foodstuff sample preparation technologies for tetracycline residue determination, Talanta 182 (2018) 1–21, https://doi.org/10.1016/j.talanta.2018.01.058.

[24] M. Küçük, B. Osman, E.T. Özer, Dummy molecularly imprinted polymer-based solid-phase extraction method for the determination of some phthalate monoesters in urine by gas chromatography–mass spectrometry analysis, J. Chromatogr. A 1713 (2024) 464532, https://doi.org/10.1016/j.chroma.2023.464532.

[25] W.J. Cheong, S.H. Yang, F. Ali, Molecular imprinted polymers for separation science: a review of reviews, J. Sep. Sci. 36 (2013) 609–628, https://doi.org/10.1002/jssc.201200784.

[26] M. Arabi, A. Ostovan, A.R. Bagheri, X. Guo, L. Wang, J. Li, X. Wang, B. Li, L. Chen, Strategies of molecular imprinting-based solid-phase extraction prior to chromatographic analysis, TrAC Trends Anal. Chem. 128 (2020) 115923, https://doi.org/10.1016/j.trac.2020.115923.

[27] H. Zhang, Molecularly imprinted nanoparticles for biomedical applications, Adv. Mater. 32 (2020) 1806328, https://doi.org/10.1002/adma.201806328.

[28] E. Semenzin, E. Lanzellotto, D. Hristozov, A. Critto, A. Zabeo, E. Giubilato, A. Marcomini, Species sensitivity weighted distribution for ecological risk assessment of engineered nanomaterials: the n-TiO2 case study, Environ. Toxicol. Chem. 34 (2015) 2644–2659, https://doi.org/10.1002/etc.3103.

[29] A. Denizli, R. Say, B. Garipcan, S. Patır, Methacryloylamidoglutamic acid functionalized poly (2-hydroxyethyl methacrylate) beads for UO22+ removal, React. Funct. Polym. 58 (2004) 123–130, https://doi.org/10.1016/j.reactfunctpolym.2003.09.005.

[30] E. Yeşilova, B. Osman, A. Kara, E.T. Özer, Molecularly imprinted particle embedded composite cryogel for selective tetracycline adsorption, Sep. Purif. Technol. 200 (2018) 155–163, https://doi.org/10.1016/j.seppur.2018.02.002.

[31] G. Aylaz, M. Andaç, A. Denizli, M. Duman, Recognition of human hemoglobin with macromolecularly imprinted polymeric nanoparticles using non-covalent interactions, J. Mol. Recognit. 34 (12) (2021) e2935, https://doi.org/10.1002/jmr.2935.

[32] S. Akgönüllü, H. Yavuz, A. Denizli, SPR nanosensor based on molecularly imprinted polymer film with gold nanoparticles for sensitive detection of aflatoxin B1, Talanta 219 (2020) 121219, https://doi.org/10.1016/j.talanta.2020.121219.

[33] B. Osman, L. Uzun, N. Beşirli, A. Denizli, Microcontact imprinted surface plasmon resonance sensor for myoglobin detection, Mater. Sci. Eng. C 33 (Issue 7) (2013) 3609–3614, https://doi.org/10.1016/j.msec.2013.04.041.

[34] X. Wie, A. Samadi, S.M. Husson, Synthesis and characterization of molecularly imprinted polymers for chromatographic separations, Sep. Sci. Technol. 40 (2005) 109–129, https://doi.org/10.1081/SS-200041880.

[35] G. Krishnamoorthy, E.T. Carlen, A. Van Der Berg, R.B.M. Scasfoort, Surface plasmon resonance imaging based multiplex biosensor: integration of biomolecular screening detection and kinetics estimation, Sens. Actuat. B. 148 (2010) 511–521, https://doi.org/10.1016/j.snb.2010.04.015.

[36] E. Agadellis, A. Tartaglia, M. Locatelli, A. Kabir, K.G. Furton, V. Samanidou, Mixed-mode fabric phase sorptive extraction of multiple tetracycline residues from milk samples prior to high performance liquid chromatography-ultraviolet analysis, Microchem. J. 159 (2020) 105437, https://doi.org/10.1016/j.microc.2020.105437.

[37] Y. Zhao, X. Gu, S. Gao, J. Geng, X. Wang, Adsorption of tetracycline (TC) onto montmorillonite: cations and humic acid effects, Geoderma 183–184 (2012) 12–18.

[38] A. Abbas, M.J. Linman, Q. Cheng, Sensitivity comparison of surface plasmon resonance and plasmon-waveguide resonance biosensors, Sens. Actuat. B. 156 (2011) 169–175, https://doi.org/10.1016/j.snb.2011.04.008.

[39] S. Zeb, A. Wong, S. Khan, S. Hussain, M.D. Sotomayor, Using magnetic nanoparticles/MIP-based electrochemical sensor for quantification of tetracycline in milk samples, J. Electroanal. Chem. 900 (2021) 115713, https://doi.org/10.1016/j.jelechem.2021.115713.

[40] N. Liang, X. Hu, W. Li, Y. Wang, Z. Guo, X. Huang, Z. Li, X. Zhang, J. Zhang, J Xiao, X. Zou, J. Shi, A dual-signal fluorescent sensor based on MoS2 and CdTe quantum dots for tetracycline detection in milk, Food Chem 378 (2022) 132076, https://doi.org/10.1016/j.foodchem.2022.132076.

[41] J. Hou, H. Li, L. Wang, P. Zhang, T. Zhou, H. Ding, L. Ding, Rapid microwave-assisted synthesis of molecularly imprinted polymers on carbon quantum dots for fluorescent sensing of tetracycline in milk, Talanta 146 (2016) 34–40, https://doi.org/10.1016/j.talanta.2015.08.024.

[42] X. Liu, S. Zheng, Y. Hu, Z. Li, F. Luo, Z. He, Electrochemical immunosensor based on the chitosan-magnetic nanoparticles for detection of tetracycline, Food Anal. Method. 9 (2016) 2972–2978, https://doi.org/10.1007/s12161-016-0480-z.

[43] A. Mohammad-Razdari, M. Ghasemi-Varnamkhasti, S. Rostami, Z. Izadi, A. A. Ensafi, M. Siadat, Development of an electrochemical biosensor for impedimetric detection of tetracycline in milk, J. Food Sci. Technol. 57 (2020) 4697–4706, https://doi.org/10.1007/s13197-020-04506-2.

[44] W. Hou, Z. Shi, Y. Guo, X. Sun, X. Wang, An interdigital array microelectrode aptasensor based on multi-walled carbon nanotubes for detection of tetracycline, Bioprocess Biosyst. Eng. 40 (2017) 1419–1425, https://doi.org/10.1007/s00449-017-1799-6.

[45] X. Ma, C. Du, J. Zhang, M. Shang, W. Song, A system composed of vanadium (IV) disulfide quantum dots and molybdenum (IV) disulfide nanosheets for use in an aptamer-based fluorometric tetracycline assay, Microchim. Acta 186 (2019) 1–7, https://doi.org/10.1007/s00604-019-3983-7.

[46] W. Gao, P. Li, S. Qin, Z. Huang, Y. Cao, X. Liu, A highly sensitive tetracycline sensor based on a combination of magnetic molecularly imprinted polymer nanoparticles and surface plasmon resonance detection, Microchim. Acta 186 (2019) 1–8, https://doi.org/10.1007/s00604-019-3718-9.

[47] Z.Q. Jiang, H. Cai, X.Y. Zhang, J.Ping Wang, Determination of tetracyclines in milk with a molecularly imprinted polymer-based microtiter chemiluminescence sensor, Anal. Lett. 52 (2019) 1315–1327, https://doi.org/10.1080/00032719.2018.1537282.

[48] J. Wang, S. Wang, K. Zhang, F. Liu, Q. Du, A metal-organic framework-based sensor for specific detection of tetracycline in milk, J. Mol. Struct. 1309 (2024) 138152, https://doi.org/10.1016/j.molstruc.2024.138152.

[49] M. Bai, F. Yue, S. Zhai, M. Hu, G. Qi, S. Chen, B. Li, X. Sun, Y. Guo, G. Marrazza, Screening of broad-spectrum aptamers to construct an electrochemical aptasensor for the sensitive detection of tetracycline antibiotic residues in milk, Sens. Actuat. B Chem. 398 (2024) 134765, https://doi.org/10.1016/j.snb.2023.134765.

[50] M. Amjadi, J.L. Manzoori, F. Pakpoor, Photometric determination of tetracycline based on surface plasmon resonance of silver nanoparticles, J. Anal. Chem. 71 (2016) 253–258, https://doi.org/10.1134/S1061934816030072.



Monireh Bakhshpour-Yucel is an associate professor at the Chemistry Department, Bursa Uludag University, Turkey. She received her Ph.D. in 2016 from the Chemistry Department at Hacettepe University. She focuses on designing and developing sensor systems, including Surface Plasmon Resonance, Quartz Crystal Microbalance, and interferometric refractive imaging sensors, for the detection of pathogenic microorganisms and cancer cells, and also synthesis and characterization of the polymeric matrix, purification, and isolation of biomolecules.



Melike Küçük graduated from Bursa Uludag University, Department of Chemistry in 2020. She received her master's degree at the same institute. She is a research assistant at Bursa Uludag University, Department of Chemistry. Her main research fields are polymeric nanomaterials and analytical separation techniques.



Elif Tümay Özer received her Master's degree in 2003 and her Ph.D. in 2010 from the Analytical Chemistry Division of the Chemistry Department at Bursa Uludağ University. She is a professor at the Chemistry Department, Bursa Uludağ University, Bursa, Turkey. She focuses on method development of chromatographic systems, including gas and liquid chromatography, and synthesis and characterization of the polymeric adsorbents for purification and separation of harmful environmental molecules.



Bilgen Osman is a professor at Bursa Uludağ University in Bursa, Turkey. She completed her doctoral studies at the same university, the Department of Chemistry, in 2011. Her research focuses on the synthesis and applications of molecularly imprinted polymers and surface plasmon resonance sensor systems.